

Lawrence Berkeley National Laboratory

LBL Publications

Title

Highly Flexible and Stretchable Nanowire Superlattice Fibers Achieved by Spring-Like Structure of Sub-1 nm Nanowires

Permalink

<https://escholarship.org/uc/item/3q4508g7>

Journal

Advanced Functional Materials, 29(39)

ISSN

1616-301X

Authors

Zhang, Simin
Lin, Haifeng
Yang, Haozhou
[et al.](#)

Publication Date

2019-09-01

DOI

10.1002/adfm.201903477

Peer reviewed

Highly Flexible and Stretchable Nanowire Superlattice Fibers Achieved by Spring-Like Structure of Sub-1 nm Nanowires

Simin Zhang, Haifeng Lin, Haozhou Yang, Bing Ni, Haoyi Li, and Xun Wang*

Conventional inorganic nanowire (NW) fibers are usually not stretchable and elastic, which may limit their practical applications. Inspired by the similarity between inorganic sub-1 nm NWs and polymer chains in dimension, and helical spring-like structure of cellulose in cherry bark, highly flexible and stretchable NW superlattice fibers composed of sub-1 nm GdOOH NWs are fabricated. The NW fibers could be twined, bent, twisted, and tied without any damage. When the strain is less than 10%, the fibers present elastic deformation. The elongation at break of the fibers usually reaches $\approx 40\text{--}50\%$ and the highest elongation could reach $\approx 86\%$. Excellent flexibility and stretchability of the NW fibers are attributed to the well-aligned spring-like NWs assembled superlattice, which are demonstrated by scanning electron microscopy tests, synchrotron small-angle X-ray scattering, and obvious birefringence. Moreover, NW-nanoparticle (NP) fibers are fabricated, inspired by inorganic nanoparticle-reinforced polymers. The strength is improved compared with the NW fibers. Based on this work, it is possible to fabricate multifunctional, flexible, and stretchable inorganic NW materials composed of different inorganic sub-1 nm NWs, which may be useful in practical applications.

chains from the viewpoint of dimension, wet-spinning and electrospinning method which are often applied in the polymer field^[3] are extended to fabricate the NW fibers and found efficient.^[4] It is reported that the Bi_2S_3 , Au, and hydroxyapatite (HAP) NW fibers etc. could be obtained via the wet-spinning method and the GdOOH NW fibers etc. could be obtained via the electrospinning method.^[5] They had good application prospects, displaying good optical or mechanical properties. But the NW fibers obtained so far are not so stretchable, and the elongation at break is low. There is a lack of proper hierarchical structures to achieve highly flexible and stretchable NW fibers. Kayoko Kobayashi et al. found the cherry bark's characteristically hierarchical structure, which provides a new idea for fabricating flexible and stretchable NW materials.^[6] It is worth noting that cellulose in nature generally makes material brittle and hard,

1. Introduction


Recently, various inorganic ultrathin nanowires (NWs) are synthesized, and they exhibit numerous applications in optical, electrical, and magnetic fields.^[1] In order to expand the performance levels, various methods are developed to translate the properties inherent in ultrathin NWs into the macroscopic structures for practical applications, such as microfluidic technique, Langmuir–Blodgett (LB) technique, Langmuir–Schaeffer (LS) technique, and epitaxial method.^[2] Considering that ultrathin inorganic NWs are structurally similar to polymer

but cellulose fibers folded like helical springs make cherry bark ultratough. For sub-1 nm NWs, which are similar to cellulose fibers, curved and flexible in the dispersions, conducting them through an appropriate method to fabricate elastic and flexible materials is hopeful. As to the fabrication method, wet-spinning is a kind of powerful technique to process NWs and the compositions of the spinning dope and coagulation bath, flow rate etc. have great impact on the fibers fabricated, because they will influence the injection stress, shear force, and solvent exchange.^[7] The polymer chains-like sub-1 nm NWs should be able to be processed into rather stretchable and flexible materials via wet-spinning method by properly conducting the spinning dope and flow field.

In this work, sub-1 nm GdOOH NWs and nanoparticles (NPs) were synthesized according to a facile solvothermal method reported by our group.^[8] The NW fibers were fabricated by injecting the well-dispersed and highly viscous spinning dope into a coagulation bath. Thus some highly stretchable and flexible NW fibers were obtained. The elongations at break of the NW fibers usually reached 40–50% and the highest elongation could reach $\approx 86\%$. In addition, the NW fibers are highly flexible. They could be twined, bended, twisted, and tied without any crack. Then the mechanism was investigated by the structural transformation and synchrotron small-angle X-ray scattering (SAXS) during tensile test. The results indicated that

S. Zhang, H. Yang, Dr. B. Ni, Dr. H. Li, Prof. X. Wang
Key Lab of Organic Optoelectronics and Molecular Engineering
Department of Chemistry
Tsinghua University
Beijing 100084, China
E-mail: wangxun@mail.tsinghua.edu.cn

Prof. H. Lin
Key Laboratory of Eco-Chemical Engineering
College of Chemistry and Molecular Engineering
Qingdao University of Science and Technology
Qingdao 266042, China

 The ORCID identification number(s) for the author(s) of this article can be found under <https://doi.org/10.1002/adfm.201903477>.

DOI: 10.1002/adfm.201903477

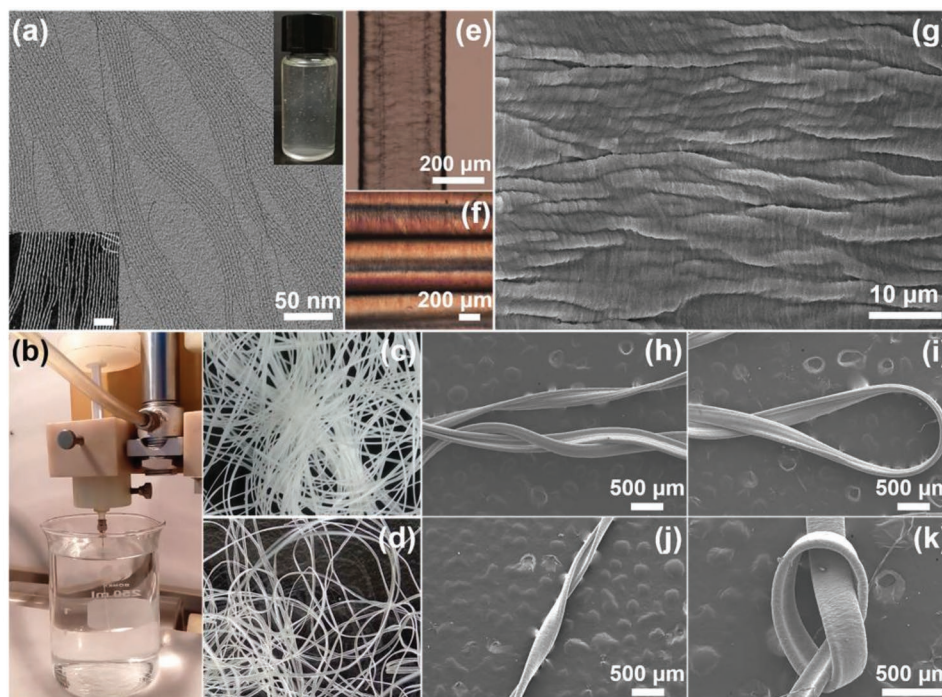


Figure 1. The fabrication process and morphology characterization of the GdOOH NW fibers. a) The TEM image and the STEM image (inset bottom left, the scale bar is 20 nm) of sub-1 nm GdOOH NWs. The photograph (inset up right) shows the dispersion of NWs. b) The preparation process of the NW fibers. c) The photograph of gel NW fibers. d) The photograph of dried NW fibers. e) The optical microscopy image of a NW fiber. f) The optical image of the NW fibers under polarizing microscope with crossed polarizers. The angle between the axis of the NW fibers and polarization direction of analyzer was 0° . g) SEM image of a NW fiber at high magnification. h–k) SEM images of the twined, bended, twisted, and tied NW fibers.

the well-aligned spring-like NWs assembled superlattice in the fibers were main inducements. Moreover, NW–NP fibers were fabricated to reinforce and toughen the NW fibers, encouraged by the inorganic NPs reinforced polymers. Our work takes advantage of the similarities between sub-1 nm NWs and polymers, fabricating highly stretchable and flexible NW fibers and reinforces the NW fibers by learning from the inorganic NPs reinforced polymers.

2. Results and Discussion

Transmission electron microscopy (TEM) image (Figure 1a) and scanning transition electron microscope (STEM) image (bottom left inset image) showed that the GdOOH NWs were with lengths of hundreds of nanometers and diameters of sub-1 nanometer. After shaking, there were lots of bubbles trapped in the dispersion of NWs (the upright inset image in Figure 1a), indicating its high viscosity. Then the slurry of NWs dispersed in octane was prepared as the spinning dope. Figure 1b displayed the automated preparation process of the NW fibers by simply injecting the prepared spinning dope into a coagulation bath containing absolute ethanol and octane (3:1 v/v) through a round-end needle with an inner diameter of 0.88 mm, using a syringe pump to control the rate. As to the synthetic mechanism of the NW fibers, the multiple forces on the NWs during the fabrication process were crucial. At first, the wet-spinning dope flowed into the syringe needle under injection stress, and a prealignment formed. The shear force was relatively effective

in this process. Subsequently, the wet-spinning dope flowed through the syringe needle and immersed in the coagulation bath. The NWs shrank and aligned under the effect of solvent exchange and gravity. The tensile force induced by gravity, pressure induced by solvent exchange, and shear force led to the formation of the NW fibers. In order to fabricate highly flexible and stretchable NW fibers, the compositions of the spinning dope were regulated. The NW fibers fabricated without addition of tetrabutylammonium bromide (TBAB) were shown in Figure S1 of the Supporting Information, which were white and opaque. And the NWs were nearly straight in the fibers. The NW fibers fabricated with addition of TBAB were shown in Figure 1c,d. A large scale of white gel fibers could be obtained instantly, and the fibers transformed to transparent when they were dried, which was demonstrated by the optical images (Figure 1e). As shown in Figure 1f, the NW fibers showed obvious birefringence under polarizing microscope with crossed polarizers, indicating the good alignment of NWs.^[2b,9] The SEM image in Figure 1g showed the wavy and spring-like NWs aligned well, composing the NW fibers and the magnified scanning electron microscopy (SEM) image was shown in Figure S2a (Supporting Information). Thus, the addition of TBAB was important for the formation of this kind of structure, which might had great effect on the pattern of the NWs and the interaction force between NWs. Moreover, the TBAB was equal to a solubilizer in the wet-spinning dope. The dispersion of the NWs became clearer obviously when TBAB was adding in our experimental process and it improved the dispersion of NWs. Figure 1h–k displayed that the NW fibers were sufficiently

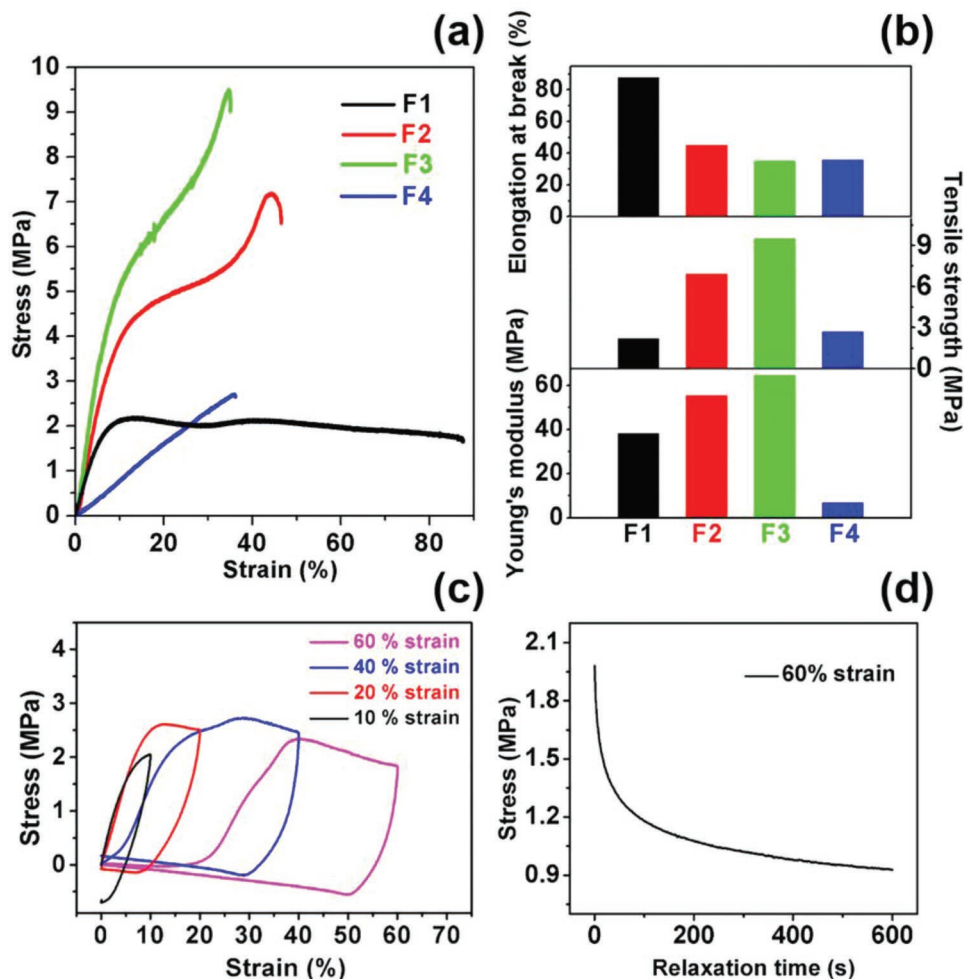


Figure 2. Mechanical properties of the NW fibers. a) The representative stress–strain curves of samples. b) The comparison of mechanical parameters of F1, F2, F3, and F4. c) The strain cycling behavior of freestanding F1. d) The relaxation behavior of freestanding F1 at the 60% strain.

flexible to be twined, bended, twisted, and tied into knots, and there was no damage to the NW fibers.

To investigate the mechanical properties of the NW fibers composed of aligned spring-like NWs, the stress–strain curves, strain cycling behavior, and relaxation behavior were tested. And in order to investigate the influence of spinning dope and coagulation bath on NW fibers, we fabricated F1, F2, F3, and F4. F1 (Figure 1g) represents the fibers prepared using a 70 wt% spinning dope at a rate of 0.012 mm s^{-1} , and the coagulation bath is a mixture of ethanol and octane (3:1 v/v). F2, F3, and F4 (Figure S3, Supporting Information) represent the fibers prepared using a 55 wt% spinning dope at a rate of 0.012 mm s^{-1} , and the coagulation baths are the mixtures of ethanol and octane with a volume ratio of 3:1, 2:1, and complete ethanol, respectively. Representative stress–strain curves of the NW fibers spun using various spinning dopes or coagulation baths were compared in Figure 2a. It is worth noting that the elongation behavior of F1 is similar to plastic films. The stress decreased after the yield point and then increased again in the plastic region. The comparison of mechanical properties of different samples was summarized in Figure 2b. It is evident from the results that the employed spinning dope

and coagulation bath influence the mechanical properties of the NW fibers significantly. F1 showed the highest elongation of $\approx 86\%$ but the lowest tensile strength of $\approx 2.2 \text{ MPa}$. When the coagulation bath was the same with F1 and the concentration of NWs in the spinning dope decreased to 55 wt%, the elongation of the samples (F2) decreased to $\approx 48\%$, but the Young's modulus and tensile strength were both increased. It was demonstrated that appropriate increase of the concentration of the spinning dope contributed to the stretchability of the NW fibers, but was bad for the strength. Comparing the mechanical properties of F2, F3, and F4, it was found that when the spinning dope was with a concentration of 55 wt%, the Young's modulus decreased with the increased amount of absolute ethanol in the coagulation bath. As shown in Figure S4 of the Supporting Information, the winding structures are denser in F4, and then F2. The NWs in F3 are straighter than F2 and F4 and there are fewer defects in F3. Too much ethanol in coagulation bath would lead to rapid contraction of NWs so they could not be arranged well, but without absolute ethanol in coagulation bath, the structures cannot be compact. So it is important to control the ratio of octane and absolute ethanol in coagulation bath to achieve an appropriate solvent exchange.

To further investigate the mechanical properties of the NW fibers, cyclic stress–strain hysteresis and stress relaxation studies were performed. The tested cyclic stress–strain hysteresis of F1 was shown in Figure 2c. It could be seen that there was no significant permanent deformation when the strain of the NW fibers was 10%, because they presented elastic deformation. When the strain reached 20%, the permanent deformation was obvious and reached 8%, and when the strain reached 40%, the permanent deformation even reached 30%. Stress relaxation of F1 (Figure 2d) was tested to measure the viscoelastic behavior of the NW fibers. With this test, the NW fiber was strained to 60% strain. Then the stress necessary to maintain 60% strain was measured as a function of time and the stress was found to decrease with time because of NWs relaxation process that took place within the fibers. Based on polymer mechanics, it is relatively easy to understand the relaxation behavior of the NW fiber. In the first stage, there was a rapid “plastic relaxation,” and it was a result of high NWs mobility produced by load-bearing segments.^[10] During this stage, the NWs slid and tried to recover the spring-like state. Then the tension dropped and could not keep the segments activated, so the stress decrease became logarithmically slow. The stress relaxation of the NW fibers was obvious with stress down by more than half.

The NW fibers stretched to different strains were studied by SEM in order to understand the failure mechanism. The distinction of the NW fibers in the natural state and in tension was clearly shown in Figure 3a–c. When the NW fiber was stretched, the spring-like NWs nearly transformed to straight, orienting in the direction of stress. The onset of elastic deformation for NW fibers resulted from NWs in curved state elongating in the direction of the applied tensile stress. The transition from elastic to plastic deformation occurred when adjacent NWs slid past one another and the NWs became more aligned in the tensile direction. The NWs displacement was resisted by van der Waals force and friction. When stress reached the yield point, shear band (Figure 3d) appeared which was similar to polymer. And within the shear band, the NWs became aligned parallel to the elongation direction. Subsequently the NWs completely separated and the fibers cracked. As shown in Figure 3e, the NWs recovered the spring-like state. The cross-section of the NW fiber after tensile fracture was shown in Figure 3f,g. There was necking phenomenon on the cross-section and the ordered holes were induced by the pulling of the NWs bundle during tensile fracture. Figure 3h showed the SEM image of a helical fiber, and the SEM images of the outer surface (Figure 3i) and inner surface (Figure 3j) of the helical fiber demonstrated the obvious difference of them. The outer surface was under tension condition and the NWs in the outer surface were straight, while the inner surface was under compression condition and the NWs in the inner surface were highly curved. Figure 3k displayed the tensile process of the NW fibers. The NW fibers reported here showed high stretchability and flexibility because of their unusual structure. The well-aligned and curved sub-1 nm NWs composing the fibers were alike to some tiny springs. When the NW fibers were stretched uniaxially, the spring-like NWs elongated and straightened first, and there might be a little slide between them. After

the NWs elongated to the limit, completely straightening, the NWs mainly overcame van der Waals force and friction to slide until the NWs completely separated and the fibers cracked. The representative stress–strain curve of NW fibers fabricated without addition of TBAB was shown in Figure S3 of the Supporting Information, showing low stretchability. When they were stretched uniaxially, the NWs overcame van der Waals forces and friction to slide until the NWs completely separated without the process from curved to straight and there was no necking phenomenon (Figure S6, Supporting Information). The synchrotron SAXS gave the structure information of the NW fibers in situ. The anisotropic SAXS diffusive pattern together with the obvious scattering peak indicated the spring-like NWs assembled superlattice (Figure 3i,k). As shown in Figure 3i,j, the anisotropy of SAXS 2D pattern became more pronounced in tension, indicating that the NWs showed higher degree of orientation in tension. Spring-like NWs-assembled superlattice was gradually straightened. In the integrated scattering profile (Figure 3k) derived from the SAXS, the intensity of the peaks obviously increased, which further demonstrated the enhancement of the orientation of the NWs with strain increased.^[5b,7e,11] In essence, the mechanical properties of the NW fibers mainly came from the sub-1 nm diameters, high aspect ratio, and good alignment of the NWs. And due to the spring-like structure composed of well-aligned NWs, the highly flexible and stretchable NW fibers could be obtained.

The NW-NP fibers were fabricated on the basis of F1, with the same coagulation bath and concentration of NWs in spinning dope. The GdOOH NPs were shown in Figure S7 (Supporting Information). As shown in Figure 4a–f, the morphologies of NW–NP fibers were quite different from the NW fibers. The NPs might fill in the structure, forming rather rough surface. As shown in Figure 4g,i, the tensile strength and Young’s modulus of the NW–NP fibers with 5 wt% NPs were obviously higher than F1 while the elongations decreased obviously. Comparing the mechanical parameters of NW–NP fibers with 7.5 wt% and 5 wt% NPs, when the mass percentage of the NPs increased from 5% to 7.5%, the tensile strength did not decrease while the Young’s modulus and elongation at break decreased. When the mass percentage of the NPs increased to 10%, the mechanical properties were obviously decayed which might be due to excessive aggregation of NPs. So the addition of NPs as reinforcing agents needs to be controlled. The tested strain cycling behavior of the NW–NP fibers with 5% NPs was shown in Figure 4h. The permanent deformation of the NW–NP fibers was lower than the NW fibers when they reached the same strain. Similarly, when the strain of the NW–NP fibers was 10%, the fibers presented elastic deformation. When the strain reached 20%, the permanent deformation reached 4%, and when the strain reached 40%, the permanent deformation reached 24%. It was demonstrated that adding some NPs into the NW spinning dope had good effects on the mechanical properties, which might be originated from the fill of the defects and the increase of the friction. The stretchability of the GdOOH NW fibers and NW–NP fibers is excellent compared to the inorganic NW fibers reported before, and the specific comparison is shown in Table S1 (Supporting Information).

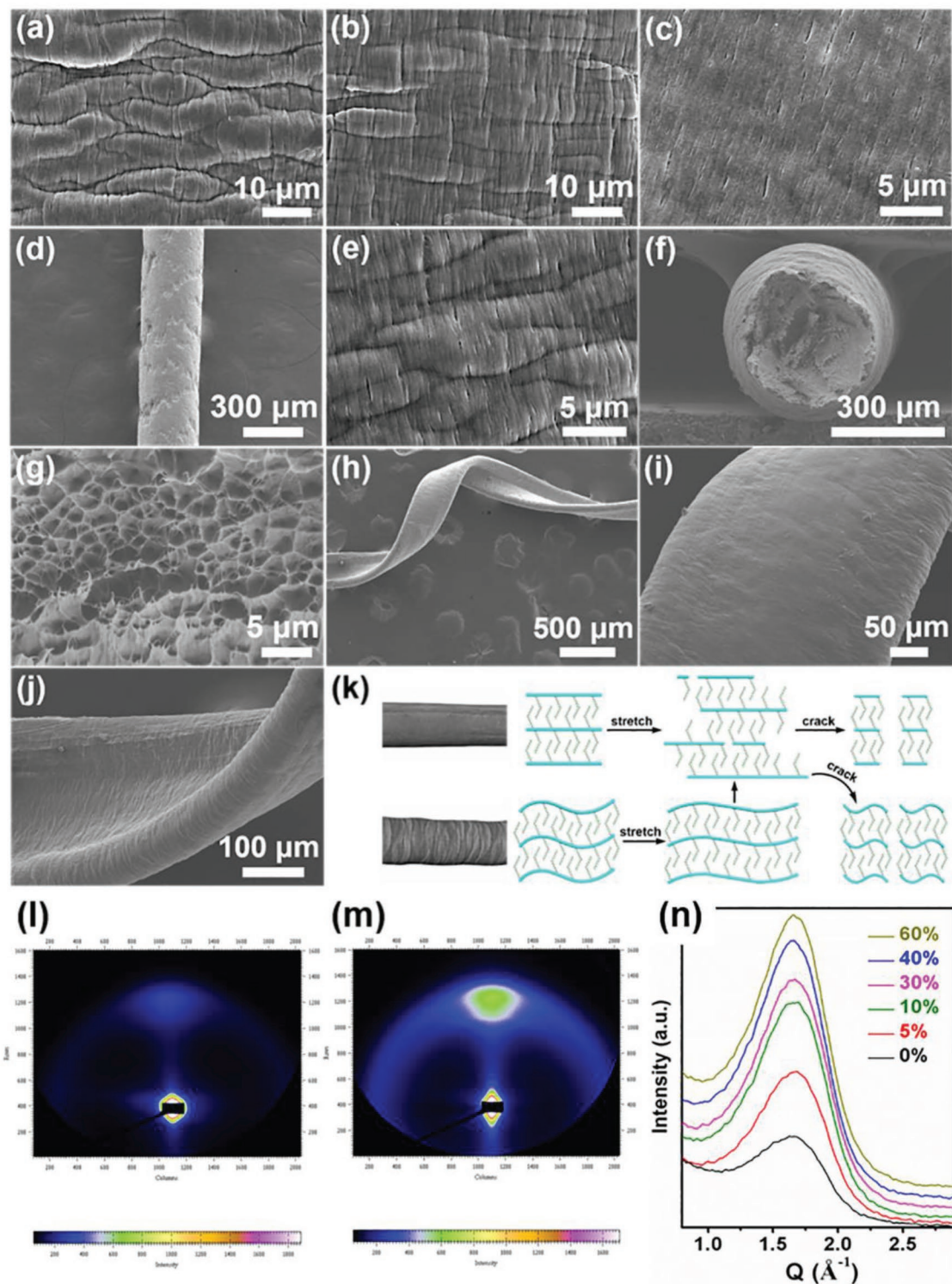


Figure 3. Characterization of the NW fibers in tension or cracked. a) The SEM image of the NW fiber in the natural state. b,c) The SEM images of the NW fiber in tension. d) SEM image of the shear bands on the NW fiber. e) The SEM image of the NW fiber after tensile fracture. f,g) SEM images of the cross-section of the NW fiber after tensile fracture. h) SEM image of a helical fiber at low magnification. SEM images of the i) outer surface and j) inner surface of the helical fiber. k) The diagram shows the tensile process of the NW fibers. l,m) Schematic depictions of the synchrotron SAXS for in situ observation of the NW fibers before and in tension. n) The integrated scattering profile derived from the SAXS.

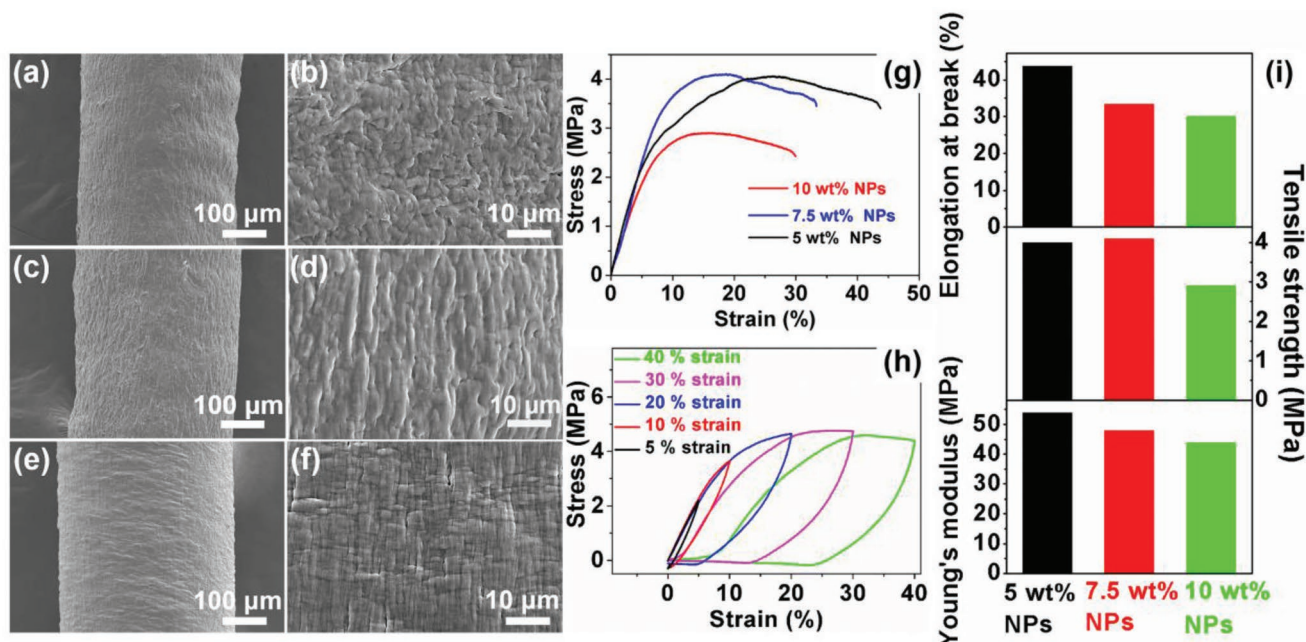


Figure 4. Mechanical properties of the NW-NP fibers. The SEM images of the NW-NP fibers with a,b) 10 wt% NPs, c,d) 7.5 wt% NPs, and e,f) 5 wt% NPs. g) The representative stress–strain curves of the NW-NP fibers. h) Strain cycling behavior of freestanding NW-NP fibers with 5 wt% NPs. i) The comparison of mechanical parameters of NW-NP fibers with 10, 7.5, and 5 wt% NPs.

3. Conclusion

In summary, highly ordered NW fibers composed of spring-like sub-1 nm GdOOH NWs were fabricated. The inorganic NW fibers fabricated via wet-spinning method are usually not so prominent in flexibility and stretchability. But in this work, the ordered spring-like NWs structure formed by controlling the spinning dope and coagulation bath, flow rate etc. properly. In addition, the NP–NW fibers were fabricated to enhance the mechanical properties of the NW fibers encouraged by the inorganic NPs reinforced polymers. And through this method, the fibers were reinforced and toughened to a certain degree. The NPs reinforced fibers provide a new idea for the reinforcement of the freestanding NW fibers and films, and through changing the compositions of the NPs, some new performances could be introduced. It is demonstrated that the ultrathin NWs are not only like polymer chains dimensionally, but also could be processed into macroscopic structures similar to flexible and stretchable polymer materials, which might provide an effective approach to process various inorganic sub-1 nm NWs for their practical applications.

Supporting Information

Supporting Information is available from the Wiley Online Library or from the author.

Acknowledgements

This work was supported by National Key R&D Program of China (2017YFA0700101, 2016YFA0202801), NSFC (21431003).

Conflict of Interest

The authors declare no conflict of interest.

Keywords

fibers, flexible, spring-like, stretchable, sub-1 nm nanowires

Received: April 30, 2019
Revised: June 28, 2019
Published online: July 28, 2019

- [1] a) H. Liu, H. Li, P. He, X. Wang, *Small* **2016**, *12*, 1006; b) J. W. Liu, J. Xu, H. W. Liang, K. Wang, S. H. Yu, *Angew. Chem., Int. Ed.* **2012**, *51*, 7420; c) J. Hui, Q. Yu, Y. Long, Z. Zhang, Y. Yang, P. Wang, B. Xu, X. Wang, *Chem. - Eur. J.* **2012**, *18*, 13702; d) D. Zhang, S. W. Eaton, Y. Yu, L. Dou, P. Yang, *J. Am. Chem. Soc.* **2015**, *137*, 9230; e) D. Zhang, Y. Yu, Y. Bekenstein, A. B. Wong, A. P. Alivisatos, P. Yang, *J. Am. Chem. Soc.* **2016**, *138*, 13155; f) N. Zhang, Z. Wang, R. Song, Q. Wang, H. Chen, B. Zhang, H. Lv, Z. Wu, D. He, *Sci. Bull.* **2019**, *64*, 540.
- [2] a) J. Lv, K. Hou, D. Ding, D. Wang, B. Han, X. Gao, M. Zhao, L. Shi, J. Guo, Y. Zheng, *Angew. Chem.* **2017**, *129*, 5137; b) O. Muskens, M. Borgström, E. Bakkers, J. Gómez Rivas, *Appl. Phys. Lett.* **2006**, *89*, 233117.
- [3] M. Richard-Lacroix, C. Pellerin, *Sci. China: Chem.* **2013**, *56*, 24.
- [4] Z. Zheng, L. Gan, T. Y. Zhai, *Sci. China Mater.* **2016**, *59*, 200.
- [5] a) L. Cademartiri, F. Scotognella, P. G. O'Brien, B. V. Lotsch, J. Thomson, S. Petrov, N. P. Kherani, G. A. Ozin, *Nano Lett.* **2009**, *9*, 1482; b) B. Reiser, D. Gerstner, L. Gonzalez-Garcia, J. H. Maurer, I. Kanelidis, T. Kraus, *ACS Nano* **2017**, *11*, 4934; c) F. Chen, Y.-J. Zhu, *ACS Nano* **2016**, *10*, 11483.
- [6] K. Kobayashi, Y. Ura, S. Kimura, J. Sugiyama, *Adv. Mater.* **2018**, *30*, 1705315.

- [7] a) A. Mirabedini, J. Foroughi, B. Thompson, G. G. Wallace, *Adv. Eng. Mater.* **2016**, *18*, 284; b) L. Kou, T. Huang, B. Zheng, Y. Han, X. Zhao, K. Gopalsamy, H. Sun, C. Gao, *Nat. Commun.* **2014**, *5*, 3754; c) N. Macroscopic, *Science* **2004**, *305*, 1447; d) R. Jalili, S. H. Aboutalebi, D. Esrafilzadeh, R. L. Shepherd, J. Chen, S. Aminorroaya-Yamini, K. Konstantinov, A. I. Minett, J. M. Razal, G. G. Wallace, *Adv. Funct. Mater.* **2013**, *23*, 5345; e) Z. Xu, C. Gao, *Nat. Commun.* **2011**, *2*, 571; f) S. Zhang, W. Shi, T. D. Siegler, X. Gao, F. Ge, B. A. Korgel, Y. He, S. Li, X. Wang, *Angew. Chem., Int. Ed.* **2019**, *58*, 8730.
- [8] S. Hu, H. L. Liu, P. P. Wang, X. Wang, *J. Am. Chem. Soc.* **2013**, *135*, 11115.
- [9] a) M. B. Sigman, B. A. Korgel, *J. Am. Chem. Soc.* **2005**, *127*, 10089; b) T. H. Han, J. Kim, J. S. Park, C. B. Park, H. Ihee, S. O. Kim, *Adv. Mater.* **2007**, *19*, 3924.
- [10] a) J. Liu, P. Lin, X. Li, S.-Q. Wang, *Polymer* **2015**, *81*, 129; b) G. A. Medvedev, J. W. Kim, J. M. Caruthers, *Polymer* **2013**, *54*, 6599; c) E. W. Lee, G. A. Medvedev, J. M. Caruthers, *J. Polym. Sci., Part B: Polym. Phys.* **2010**, *48*, 2399.
- [11] a) Y. Wang, P. B. Groszewicz, S. Rosenfeldt, H. Schmidt, C. A. Volkert, P. Vana, T. Gutmann, G. Buntkowsky, K. Zhang, *Adv. Mater.* **2017**, *29*, 1702473; b) X. Zhao, Z. Xu, B. Zheng, C. Gao, *Sci. Rep.* **2013**, *3*, 3164.